A Cryocooler Driven by Electrochemical Compressors with No Moving Parts

W. Chen, B. Cameron, S. Narayanan[1]

Creare, Hanover, NH 03755

[1]University of Southern California
Los Angeles, CA 90089

ABSTRACT

This paper reports on the development of a vibration-free cryocooler for infrared detectors. The cryocooler employs an Electro-Chemical Hydrogen Compressor (ECHC) with no moving parts for reliable, vibration-free operation. The ECHC uses an advanced anhydrous proton conducting membrane to compress hydrogen through an electrochemical process. This compressor produces high pressure ratios with no moving parts. The cryocooler also uses a unique single-pressure dilution cycle to provide cooling at temperatures significantly lower than the hydrogen Joule-Thomson (J-T) inversion temperature. This paper first reports preliminary test data from an open-cycle cryostat using argon as the refrigerant and hydrogen as the diluent.

The measured cooling power of the dilution cryostat is compared with predicted values. The paper also reports test data for the compression ratio and compression efficiency of a proof-of concept ECHC with a H_2-Ar mixture. Based on the performance data of the dilution cycle and the ECHC, the thermodynamic cycle design of the cryocooler is optimized and then the cryocooler performance is estimated. Preliminary mechanical designs for the ECHCs are also developed.

INTRODUCTION

Cryocoolers that use mechanical compressors, especially those operating at low frequencies (<1000 Hz), can produce significant vibration on spacecraft, which can cause substantial image artifacts. Mechanical compressors can also have reliability limits due to mechanical fatigue and wear. Cryocoolers with no mechanical moving parts are highly desirable because they produce no jitter and may enhance system reliability.

Current research in the area of solid-state cryocoolers focuses mainly on magnetic coolers, thermoelectric coolers (TEC), and optical coolers. So far, however, the ability of these cooling technologies to provide active cooling for a payload at about 120 K has not been demonstrated.

In a magnetic cooler, the local temperature swing associated with the magnetization and demagnetization processes is still limited to only a few kelvin, even with a very strong field swing (>3 T). At temperatures above 90 K, it is impractical to generate a large magnetic field swing (>2 T) with an electromagnet because high-temperature superconducting magnets cannot be used. Optical coolers require extremely pure materials for the cooling element, since the heat generated in the contaminants (due to nonradioactive transitions) can overwhelm the fluorescent 2 cooling. Even

Cryocoolers 18, edited by S.D. Miller and R.G. Ross, Jr.

though bulk cooling at temperatures of about 155 K and local cooling at 110 K have been demonstrated in the laboratory with fluorescent cooling in solid materials [1], research in implementing this cooling technology in practical cooling systems is still at a very early stage, and net cooling efficiency in practical applications has not been demonstrated.

For thermoelectric coolers, the electrical resistivity and the thermal conductivity of existing TEC materials are still too high, resulting in large internal joule heating and large conductive heat leaks from the hot side to the cold side of a TEC. This severely limits a TEC's efficiency and its maximum temperature difference. To the best of our knowledge, cooling temperatures below 150 K have not been demonstrated by a stand-alone TEC.

Because of these limitations in current solid-state cryocooler technologies, there is a strong need for alternative technologies to achieve efficient, vibration-free cooling at temperatures below 123 K while rejecting heat at significantly higher temperatures.

Creare is in the process of developing an efficient cryocooler driven by ECHCs with no mechanical moving parts. This work is built on prior work that aims to develop a 35 K cryocooler.[2,3] The cryocooler provides cooling at temperatures below 123 K and rejects heat at temperatures above 300 K. The cryocooler technology uses proven technologies that are far more mature than other current solid-state cryocooler technologies. The operations of the ECHC compressor, the operation of the cryocooler, and the predicted performance of the near-term brassboard prototype system are discussed in the following sections.

ECHC CONCEPT DESCRIPTION

In an ECHC, low-pressure hydrogen is first ionized at the anode by removing its electrons. The resulting protons are then pulled across the membrane through a voltage potential. Finally, the protons are recombined with their electrons at the cathode to form high-pressure hydrogen (Fig. 1).

The most critical component in the ECHC is the proton conducting membrane. The membrane must have a high proton conductivity to minimize parasitic voltage drop across the membrane. The total cell voltage of an electrochemical hydrogen compressor consists of the Nernst potential and the parasitic potentials, which include the total polarization voltage at the anode and cathode and the ohmic voltage drop.

For contamination-free operation, the proton conducting membranes in the ECHC must be anhydrous (water-free). The potential performance degradation modes for this type of membrane include: (1) the possibility of pinhole formation due to thinning of the membrane, which leads to increased cross-stream leakage and reduced compression efficiency, and (2) acid evaporation. Based on the performance data in fuel cell applications, the membrane in ECHC is expected to achieve a service life of higher than 20,000 hours at 160°C (433 K).

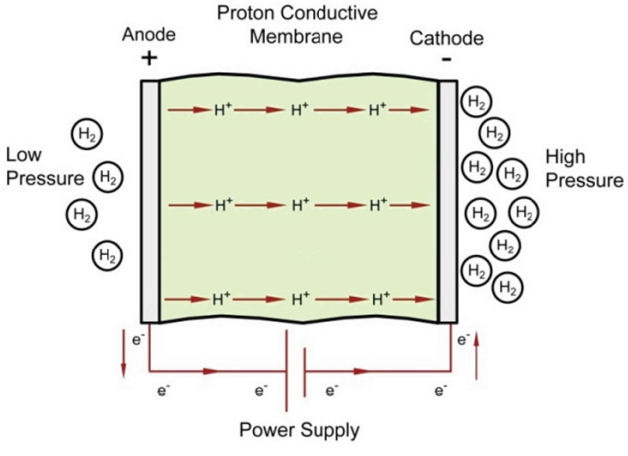

Figure 1. Operating mechanism of electrochemical H_2 compressor.

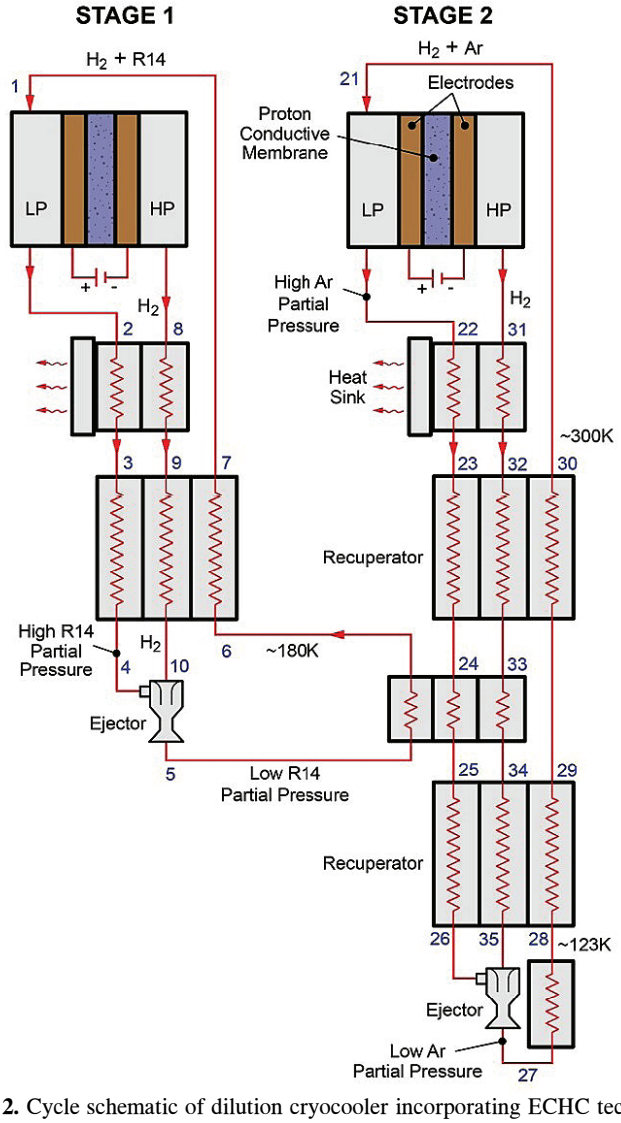

Figure 2. Cycle schematic of dilution cryocooler incorporating ECHC technology.

DILUTION CRYOCOOLER CONCEPT DESCRIPTION

A cycle schematic of a cryocooler incorporating the ECHC technology is shown in Fig. 2. The proposed cryocooler utilizes a unique two-stage dilution cycle that uses inert gases, fluoromethane, and argon as the refrigerants for upper and lower stages, respectively, and hydrogen gas as the diluent.

The total gas pressures in each dilution stage are nominally the same everywhere. Hydrogen is used to change the partial pressure of the refrigerant in the mixed gas, while the hydrogen partial pressure, in turn, is controlled by the ECHC. On the anode side (low hydrogen partial pressure side denoted "LP") of the ECHC, hydrogen is pumped out of the hydrogen-refrigerant mixture as it flows from the inlet to the outlet. Consequently, the partial pressure of refrigerant gradually increases while the hydrogen partial pressure gradually decreases. This leads to a gradually increasing hydrogen pressure ratio across the membrane from the anode inlet to the outlet. The outlet pure hydrogen stream from the cathode side (denoted "HP" for high pressure), along with the refrigerant

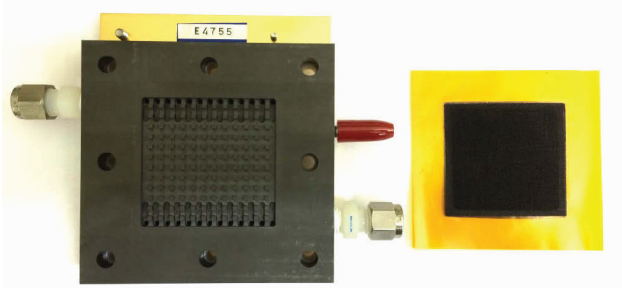

(b) Membrane-Electrode Assembly (a) Bipolar/Flow Field Plate

Figure 3. Key components in test cell for electrochemical pumping.

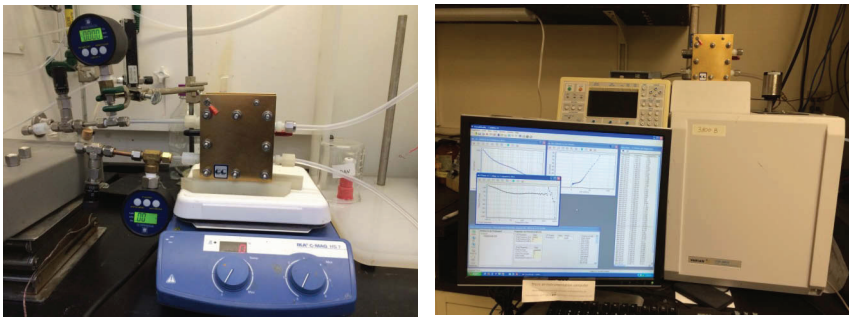

(a) Assembled compressor (b) Cell connected to gas chromatograph

Figure 4. Hydrogen membrane compressor test setup.

flow from the anode side, are precooled by the returning stream to the ECHC; then they mix together at the cold end.

During the mixing process, the partial pressure of the refrigerant is reduced significantly. This is equivalent to a J-T expansion process for the refrigerant if the Van der Waals interaction between refrigerant and hydrogen molecules is small.

In this particular application, a two-stage configuration is used to improve the system efficiency. Ejectors are used in the mixing process to allow the cathode hydrogen flow that has a slightly higher pressure than the anode outlet flow to raise the pressure of the anode flow to overcome the pressure drops in the loop (Fig. 2).

ECHC OPERATION DEMONSTRATION

A proof-of-concept single-cell ECHC was assembled to characterize its compression ratio and thermodynamic efficiency. The Membrane-Electrode Assembly (MEA) has a 25 cm^2 active area (Fig. 3). A set of commercially available bipolar/flow field plates was used to assemble the proof-of-concept H_2 compressor test setup, as shown in Fig. 4. In the first series of testing, a 50% argon and 50% hydrogen mixture was passed through the anode side of the membrane. After verifying that there is no leakage across the membrane, we gradually increased the current passing through the membrane and measured the resulting voltage across the cell, as shown in Fig. 5. We also measured the hydrogen flow rate exiting the cathode side to verify that the hydrogen flow rate matched the total current passing through the membrane (i.e., current = 2× hydrogen molar flow rate × Faraday constant), as shown in Table 1.

The test result shows that the ECHC equivalent isothermal compression efficiency decreases as the current density increases because the ohmic loss is higher. At the target current density of about 0.12 A/m^2 and an effective compression ratio of two, we can expect the efficiency of the ECHC to be about 15% — quite high for a solid-state compressor at these low power levels.

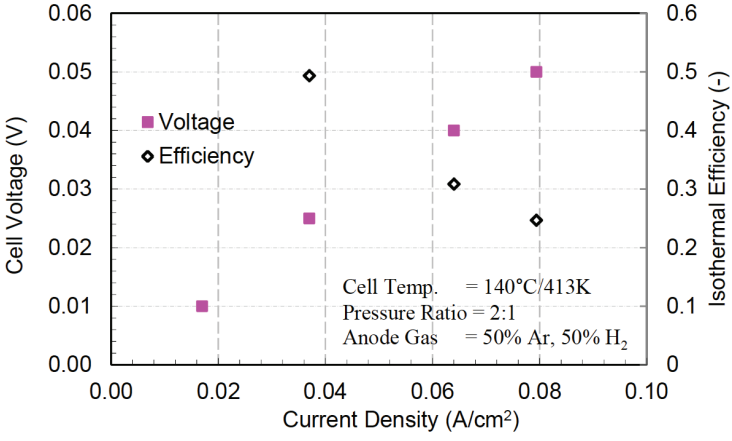

Figure 5. Cell voltage of single-cell ECHC with ambient pressure argon-hydrogen on anode side and pure hydrogen on cathode side.

Table 1. Comparison of Measured Hydrogen Flow Rate and Predicted Values based on Current.

Temperature	Steady-State Current	Measured H_2 Flow Rate on Cathode	Theoretical H_2 Flow Rate Based on SS Current
25°C	47.6 mA/cm^2	8.79 mL/min	9.04 mL/min
100°C	38.4 mA/cm^2	7.13 mL/min	7.29 mL/min
140°C	38.0 mA/cm^2	6.98L/min	7.22 mL/min

We also conducted testing with a H_2 and Ar mixture having 6.8% of H_2 at ambient pressure passing through the anode side of the cell. H_2 concentration at the anode outlet was measured by a Gas Chromatograph (GC). The result showed H_2 concentration on the anode side was reduced to 0.4 % when a current of 0.3 A was passed through the cell and hydrogen flowed out of the cathode side at ambient pressure (Fig. 6). The test results demonstrate a compression ratio of 15:1 at the anode inlet and 250:1 at the anode outlet. This result demonstrates the feasibility of the target compression ratio of about 140:1 at the anode outlet in the lower dilution stage.

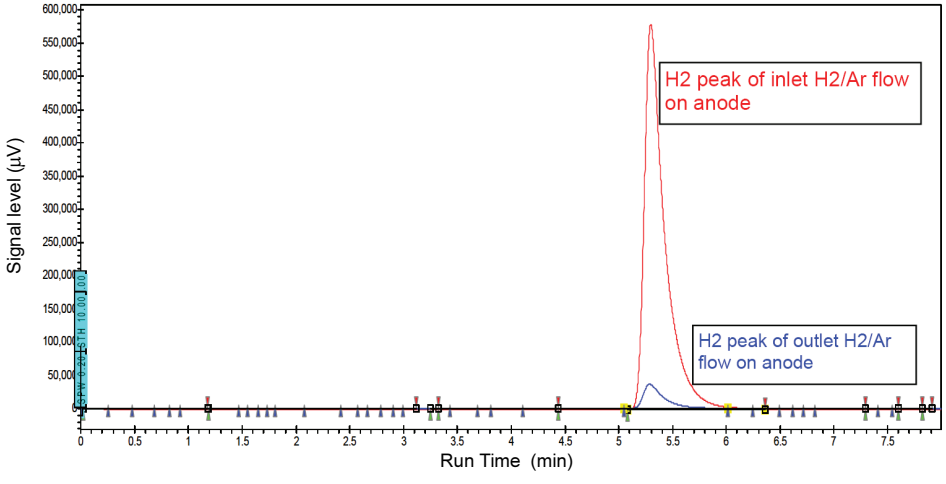

Figure 6. Anode gas analysis cell using gas chromatograph.

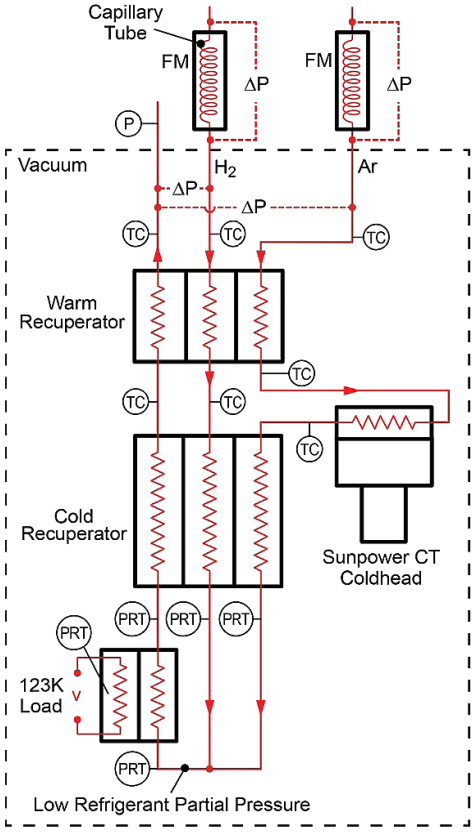

Figure 7. Dilution process test facility.

PROOF-OF-CONCEPT OPEN-LOOP DILUTION CYCLE

Test Setup

The cryogenic test setup comprises vacuum-insulated cold components located inside a bell jar and ancillary components and instrumentation located outside the bell jar at room temperature. Key components outside the bell jar include high-pressure supply gases, flow control valves, safety relief valves, dilution air to reduce H_2 concentration in the exhaust stream for safety, and flow measurement instruments. The supply gases included scientific-grade argon, hydrogen, and helium purge gas (for safety). Customized high-pressure capillary-tube mass flow meters were used to measure the flow rates of the high-pressure (about 1000 psi) gas flows. The measurement accuracy of these flow meters is about 2%.

A schematic of the cryostat inside the bell jar is shown in Fig. 7, including warm and cold recuperators, a precooler, a load heat exchanger, and temperature measurements throughout the system. A Cryotel CT cryocooler provides precooling at about 180 K, equivalent to the first stage of the system. Prior to testing we covered the system components inside the bell jar with several layers of aluminized mylar to minimize heat leaks to the cold components. Key data recorded from this test setup include flow rates of the argon and hydrogen gas streams, temperatures from the thermocouples on the warm recuperator and warm end of the cold recuperator, and temperatures from four PRT sensors on the cold end of the second dilution stage. These sensors measure the temperatures of the gases before and after mixing (dilution), and before and after passing through the load heat exchanger. We used these key temperatures, the gas flow rates, and the load heater power for performance analysis, and all other instrumentation for control and monitoring.

Due to safety concerns about a possible H_2 leak, our safety protocol prohibits use of instruments or equipment with exposed high-temperature elements, including a cathode gauge or a diffusion pump. Consequently, a small turbo-molecular vacuum pump instead of a large existing diffusion pump was use to maintain the system vacuum. Because the bell jar is quite large, the small vacuum pump can only enable the bell jar to achieve a vacuum level slightly better than 10^{-4} torr. This poor vacuum causes a relatively large heat leak into the heat load simulator during the cryogenic testing period.

TEST RESULTS

Steady-state data were collected for two different flow rates during two separate test periods to demonstrate repeatability and to compute heat leaks into the system. Key temperature data for the complete test timeline are plotted in Fig. 8, and the key steady-state results are plotted in Fig. 9.

These steady-state time periods are also shown in Fig. 8 for reference. The four plots on the top of Fig. 9 show the temperatures of the argon and hydrogen gases prior to mixing, the temperature of the gases after mixing, and the temperature of the mixed gas after passing through the load heater. The four plots at the bottom of Fig. 9 show the flow rates and load heater power during steady-state operation.

The key results from these plots are the 21 to 22 K drop in gas temperature after mixing, whereas our cycle model predicted a temperature drop of about 28 K using REFPROP 9 by NIST. To estimate the actual cooling power with an unknown heat leak into the system, we compared the change in cooling power to the load heater with the change in flow rate. This approach removed the constant heat leak power from the equation. The resulting analysis shows that the actual heat leak into the system was about 1.22 W and that the measured specific cooling power is about 0.36W/(g/min of Ar). Our cycle analysis model predicted a cooling power of about 0.44W/(g/min of Ar). This discrepancy might be due to measurement uncertainty in this preliminary test or the uncertainty in gas properties predicted by REFPROP. Note that the flow rates shown in these experiments were chosen to provide sufficient cooling to overcome the heat leak in the system and the flow rates are three to four times greater than the flow rates for the target application.

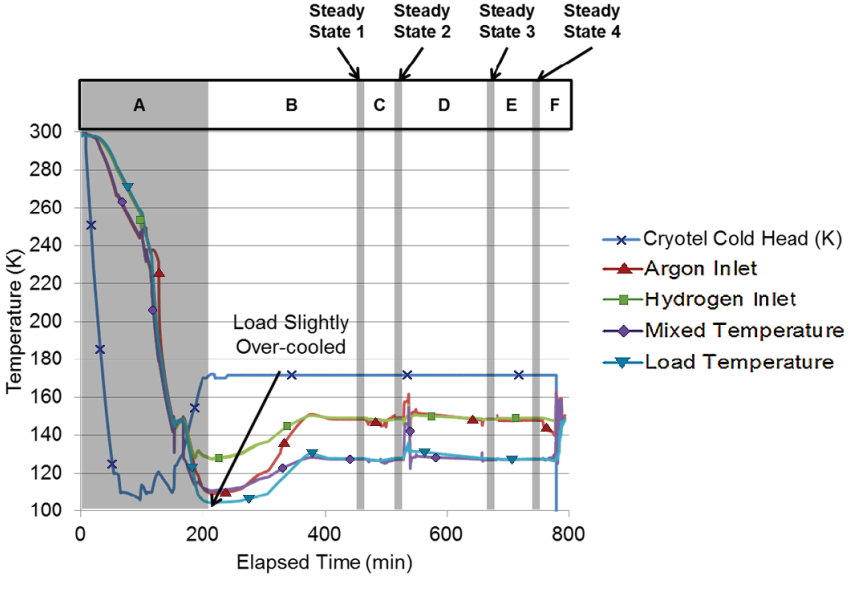

Figure 8. Proof-of-concept dilution cycle complete data set. The time periods during the test are described as follows: (A) load precooling, (B) time to reach steady-state condition 1, (C) time to reach steady-state condition 2 after flow rate is reduced, (D) time to reach steady-state condition 3 after gas bottle is changed, (E) time to reach steady-state condition 4 after flow rate is increased, and (F) system shutdown.

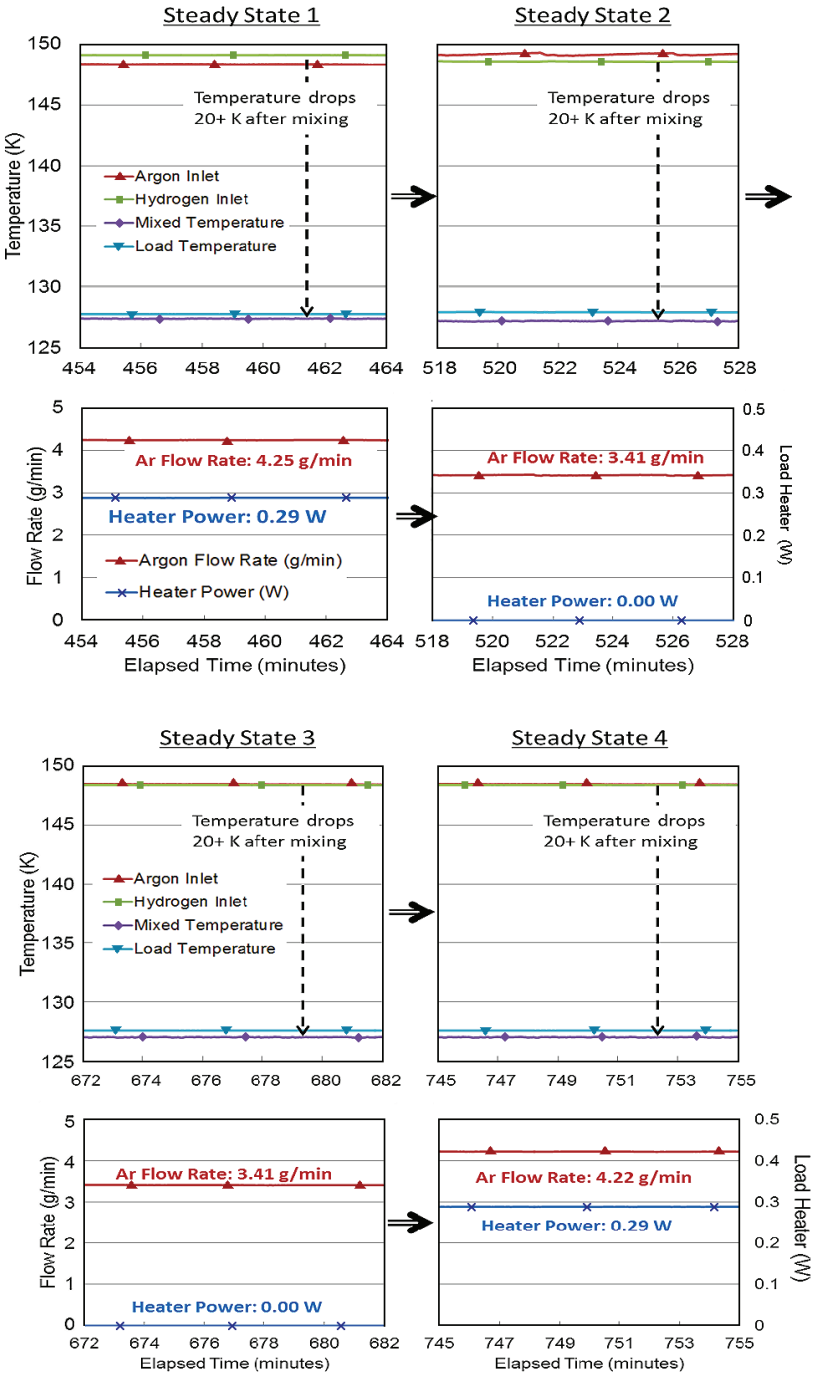

Figure 9. Proof-of-concept dilution cycle steady-state test results for two argon flow rates. The specific cooling capacity of the mixing process is determined by the change of cooling power with gas flow rates to exclude effect of heat leak.

PREDICTED NEAR-TERM PROTOTYPE SYSTEM PERFORMANCE

Based on the preliminary open-loop dilution stage test results, we updated the cycle design model to increase the refrigerant flow to compensate the slightly lower than predicted cooling capacity of the dilution process. We then developed the layout designs of the ECHC and ejector. For a cryocooler that provides 0.5 W of cooling at 123 K, the upper dilution stage needs to provide 0.35 W of precooling at 179 K for the second stage. The total system power input is about 50 W and the system mass is about 3.8 kg. These performance predictions are based on the measured performance of the proof-of-concept ECHC. Further development to increase the membrane conductivity by a factor of two (i.e., 0.05 S/cm) and reduce the bipolar plate thickness by a factor of two (500 microns) will enable the cryocooler to further reduce its mass to about 1 kg.

Finally, we devised a brassboard system design, shown in Fig. 10. Considerations in the overall layout design include trade-off between efficiency and system mass, as well as simplifying the plumbing of the cryocooler and its integration with a spacecraft. We increase the membrane current density to 0.12 A/cm^2 from the preliminary test values of about 0.08 A/cm^2 to reduce the system size and mass. The higher current density reduces the efficiency of ECHCs but the cooler specific input power is still below the target value of 100 W/W. Based on the solid model, the near-term cryocooler prototype is expected to have a mass of 3.8 kg and a size of about 2 L (0.07 ft^3). About 55% of the system mass comes from the MEA stack assembly, as shown in Fig. 11. Further improvement in the membrane conductivity will enable the ECHC to operate at a higher current density to substantially reduce the cryocooler mass.

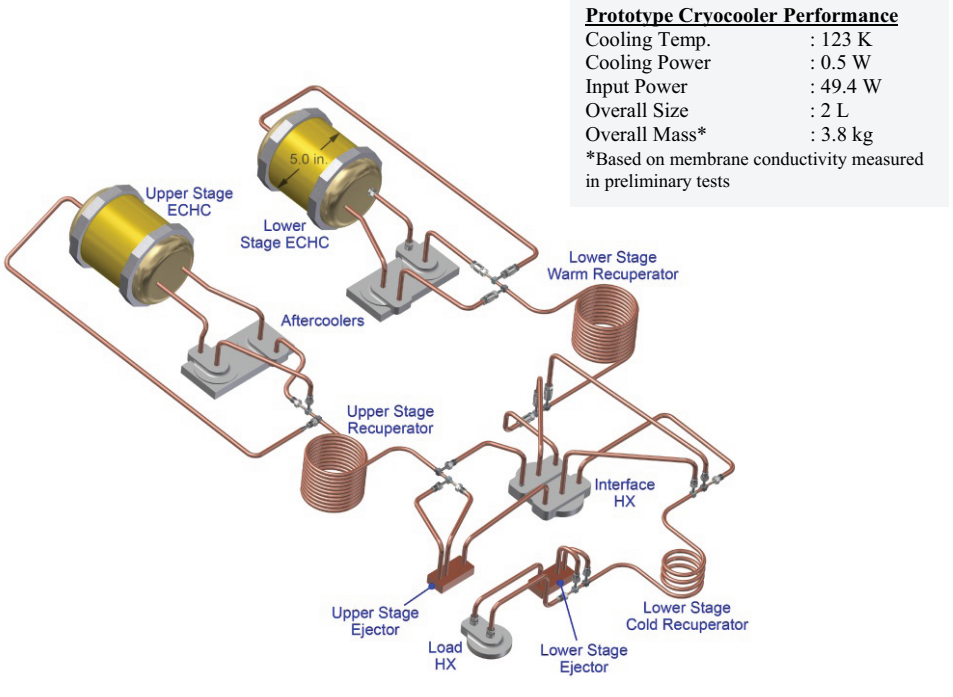

Figure 10. Preliminary layout design of brassboard dilution cryocooler incorporating ECHC technology.

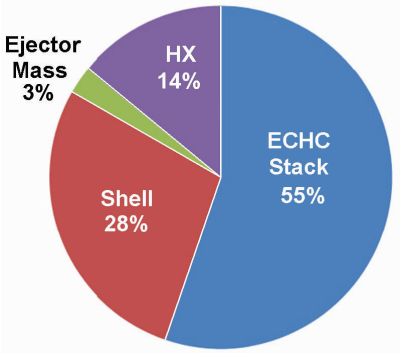

Figure 11. Mass breakdown of dilution cooler.

CONCLUSIONS

A single-cell ECHC with anhydrous membrane was assembled and demonstrated with a representative mixture with 50% argon and 50% hydrogen on its anode side. Results show that the anhydrous ECHC efficiently separated the hydrogen from the gas mixture, compressed it with a pressure ratio of higher than 2:1, which is the mass flow rate-averaged compression ratio of hydrogen in the ECHCs, and forced the resulting pure hydrogen stream out of the cathode side. The demonstrated isothermal compression efficiency is higher than 25%. A compression test with a mixture having 6% of H_2 also demonstrated that a maximum compression ratio of 250:1 can be achieved in a single-stage ECHC.

An open-loop dilution cycle cryostat was also assembled and tested with argon as the refrigerant and hydrogen as the diluent. We demonstrated a cooling temperature of about 127 K. The measured cooling capacity showed that integrated dilution cryocooler specific input power will be less (better) than 100 W/W of cooling.

Based on the test results, a brassboard dilution-cycle cryocooler driven by anhydrous ECHCs were developed. Its predicted specific input power is below 100 W/W. Its predicted mass and size are is about 3.8 kg and 2 L, respectively.

The cryocooler driven by ECHCs will enable reliable, vibration-free cryocooling for space-based surveillance, missile detection, and missile tracking. Its vibration-free operation will eliminate the need for complex, heavy active vibration cancellation systems, significantly reducing the effective size and mass of the cryocooling system.

ACKNOWLEDGMENT

The support and guidance from the Spacecraft Component Thermal Research Group, Air Force Research Laboratory, is gratefully acknowledged.

REFERENCES

1. Seletskiy, D.V., Hehlen, M.P., Epstein, R.I. and Sheik-Bahae, M., "Cryogenic Optical Refrigeration," *Advances in Optics and Photonics*, vol. 4, no. 1 (2012), pp. 78-107.
2. Chen, W., Smith, B., Zagarola, M., and Narayan, S., "A Vibration-Free 35 K Cryocooler Driven by Electrochemical Compressors," *Cryocoolers 17*, ICC Press, Boulder, CO (2012), pp. 425-433.
3. Yang, B., Manohar, A., Prakash, G.K.S., Chen, W., and Narayan, S.R., "Anhydrous Proton Conducting Membranes Based on Poly-4-Vinylpyridinium Phosphate for Electrochemical Applications," *Journal of Physical Chemistry B*, vol. 115, no. 49 (2011), pp. 14462-14468.